International Journal of Communication Networks and Information Security

ISSN: 2073-607X, 2076-0930

*Volume **14** Issue **1s Year 2022** Page **54:66***

A Broadband Meta surface Based MIMO Antenna with High Gain and Isolation For 5G Millimeter Wave Applications

Nelapati Ananda Rao[1], Lalitha Bhavani Konkyana[2], Vysyaraju Lokesh Raju[3], M.S.R. Naidu[4], Chukka Ramesh Babu[5]

[1] *Department of Electronics and Communication Engineering, Vignan's Foundation for Science Technology and Research, Andhra Pradesh, India.*

[2, 3, 4] *Department of Electronics and Communication Engineering, Aditya Institute of Technology and Management, Andhra Pradesh, India.*

[5] *Department of Electronics and Communication Engineering, Vignan's Institute of Engineering for Women, Andhra Pradesh, India.*

Article History

Received: 10 July 2022
Revised: 25 September 2022
Accepted: 20 October 2022

Abstract

This paper proposes a Broadband Meta surface-based MIMO Antenna with High Gain and Isolation For 5G Millimeter applications. A single antenna is transformed into an array configuration to improve gain. As a result, each MIMO antenna is made up of a 1x2 element array supplied by a concurrent feedline. A 9x6 Split Ring Resonator (SRR) elongated cell is stacked above the antenna to improve gain and eliminate the coupling effects between the MIMO components. The substrate Rogers 5880 with a thickness of 0.787mm and 1.6mm is used for the antenna and meta surface. Furthermore, antenna performance is assessed using S-parameters, MIMO characteristics, and radiation patterns. The final designed antenna supports 5G applications by embracing the mm-wave frequency spectrum at Ka-band, there is a noticeable increase in gain. In addition, once the meta surface is introduced, there is an improvement in isolation.

Keywords: 5G millimetre-wave, metamaterial, unit cell, MIMO Antenna, Antenna array.

1. Introduction

Wireless networks might demand 1.4 times more bandwidth in the next years than they do now, due to a massive rise in yearly data traffic. To keep up with the ever-increasing demand, Fifth-generation(5G) systems with high-demand Multigigabit per the second throughput are regarded as a key solution for upcoming application areas [1]. Communication systems are continuously expanding in the early modern era, and new features such as high throughput, fast speed, pixel density, heterogeneity, virtual servers, massively streaming data, and speedy response are attracting researchers. The emerging 5G cellular technology is also one of those communication methods. The 5G platform is built to provide a bonus pack to meet the rising demands for smartphones (transmission rate), while somehow exceeding the constraints of present communication technologies

[2-4]. The benefits of 5G networks are not only limited to achieving self-sufficiency for faster speeds or ensuring the accurate sending and receiving of data for elevating devices which are coupled to the system, they are further intended to enhance the competencies of evolving technological fields such as machine learning, building automation[5].

The primary drivers of 5G technology include arrays, MIMO, and beamforming technology. Various recent studies have looked into antenna designs for possible millimetre Wave bands. High output antenna arrays with beamforming capabilities were fully examined to solve the greater attenuation in the mm-Wave spectrum, offering enhanced signal power and large spatial coverage[6]. With 5G operations, MIMO technology is favoured to address the emerging need for improving throughput and service levels. MIMO antenna technique, was among the most essential segments of upcoming digital cellular schemes since it enhances performance without increasing voltage level or frequency band. Moreover, because of the considerable mutual interaction between neighbouring antenna components, especially when they were about a half-wavelength apart, integrating the antenna design into another chip for small-sized gadgets is difficult [7-9]. Because of the unique ability can alter electromagnetic radiation in radio frequencies, metamaterials are a significant area of attention and are employed in a multitude of scenarios. These illusionary sheet components, which are typically made up of conductive patches as well as a dielectric engraving in planar and multi-layer arrangements with sub-wavelength surface area, have the benefits of being delicate, easy to fabricate, and allowing wave propagation to be controlled both on the exterior and in the all-around free space. [10].

Several studies have described MIMO antennas employing meta surface to increase the gain of the antenna, notably coupling minimization or antenna gain enhancement. For tackling mutual coupling issues, [11] presented a 2x2 array antenna consisting of a composite Frequency Selective Surface layer. The suggested MIMO antenna gets a 6-12 dB increase in overall isolation as a result of FSS integration. Additionally, another solution is described to reduce the coupling problems in MIMO Antenna. The lengthy corners of a substrate are etched with the metamaterial-based contour in this study. As a consequence, the isolation is improved by 12-15 decibels. The given antenna has a high gain as well. However, the proposed design's substrate size is 21x85 mm, which is rather huge [12]. To improve isolation among mm-wave DRAs, a polarization-rotator is often included. This approach achieves a 16 dB decrease in mutual coupling on average [13]. For millimetre-wave applications, [14] proposes DRA with multiple designs. To improve isolation, the DRA's top side has a metamaterial structure printed on it. In an isolation between the MIMO elements, a 12-13 dB rise is found due to the inclusion of metamaterial. The operating frequency band's maximum gain is just 7 dBi, which is rather low.

This article suggests a solution to the issues mentioned. This presents a broadband meta surface-based MIMO radiator with excessive gain and good amount of isolation for 5G Millimeter wave implementation to improve gain as well as isolation. A single antenna is transformed into an array configuration to improve gain. As a result, each MIMO antenna is made up of a one-two element array supplied by a concurrent feedline. A 9x6 Split Ring Resonator (SRR) elongated cell is stacked above the antenna to improve gain and eliminate coupling effects between the MIMO components. The final designed antenna supports 5G applications by embracing the mm-wave frequency spectrum at Ka-band, there is a noticeable increase in gain. In addition, once the meta surface is introduced, there is an improvement in isolation.

2. Antenna Geometry and Design Procedure:

A 30 mm x 43 mm substrate is used to produce the suggested antenna element and MIMO antenna system with four ports. The substrate is Rogers Trademark 5880 with 0.787 mm thickness and relative permittivity of 2.2 is employed. To enhance efficiency, a meta surface array of 9x6 split ring resonator (SSR) unit cells is deployed at a height of approximately 0.5λ meters above the MIMO antenna [4]. The High-Frequency Structure Simulator tool is used for modelling and simulation. The stepwise design method, optimization techniques used, and pertinent acquired findings are all covered in detail in the following sections.

2.1 Antenna Layout:

The design modelling begins with one antenna which is displayed in Fig. 1 (a). In the first phase, often using math equations, a rectangular shaped patch antenna with feed and the surface plane is created and it is resonated at 28.9 GHz. The rectangular patch antenna is modified in the second phase by cutting arrow-shaped slots in both vertical and horizontal directions. Bow-tie antennas are commonly utilized in GPR applications. The cutting of spherical slots at all edges of antenna and the outer surface side is the last optimization process. Although there was a band shifting due to changes in antenna electrical length for three optimization phases, the total impedance transmission capacity (bandwidth) has enhanced. Table 1 presents the optimized parameters of the single antenna model.

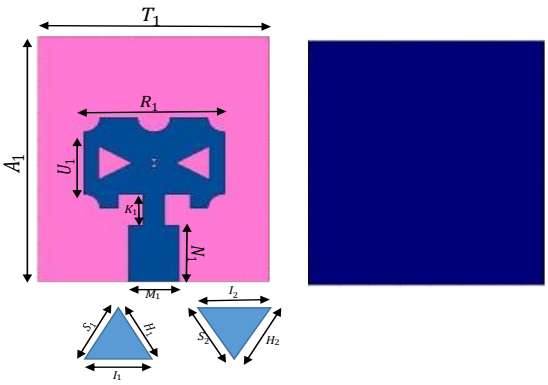

(a)

Figure1. (A) Geometry Of Single Antenna

Fig. 1 (b) shows how a single antenna is transformed into an array configuration to improve gain. The transmission line widths are determined using the characteristic equations, with the feed line impedance set to 50 and the branching network impedance set to 100Ω[15].

For $\frac{M_2}{h} \leq 1$

$$Z_O = \frac{60}{\epsilon_{reff}} ln\left(\frac{8h}{M_2} + \frac{M_2}{4h}\right)$$

Where,

$$\epsilon_{reff} = \frac{\varepsilon_r + 1}{2} + \frac{\varepsilon_r - 1}{2} \times \left(\frac{1}{\sqrt{1 + 12\frac{h}{M_2}}} + 0.004\left(1 - \frac{M_2}{h}\right)^2\right)$$

For $\frac{M_2}{h} \geq 1$

$$Z_O = \frac{120\pi\sqrt{\varepsilon_{reff}}}{\frac{M_2}{h} + 1.393 + 0.667ln\left(\frac{M_2}{h} + 1.444\right)}$$

Where,

$$\epsilon_{reff} = \frac{\varepsilon_r + 1}{2} + \frac{\varepsilon_r - 1}{2} \times \left(\frac{1}{\sqrt{1 + 12\frac{h}{M_2}}} + 0.004\left(1 - 12\frac{h}{M_2}\right)^{-\frac{1}{2}}\right)$$

where Zo is the transmission line characteristic impedance and M_2 is the feedline's width. The dielectric constant is r, and the effective permittivity is $\in_{reff}$. The formulae below are used to compute the geometrical parameters of the feed point.

$$M_2 = \frac{2h}{\sqrt{1+12\frac{h}{M_2}}}$$

$$\times\left(B-1+\frac{\varepsilon_r-1}{2\varepsilon_r}\left[\ln(B-1)+0.39-\frac{0.61}{\varepsilon_r}\right]\right)$$

$$N_2 = \frac{\lambda}{4\sqrt{\in_{reff}}}$$

$$B = \frac{60\pi^2}{Z_O\sqrt{\varepsilon_r}}$$

Here, B is a steady value employed in the equation for a microstrip line with a specified Z_0, and the feedline length is N_2. The small gap between the two array components is 1.4mm at 28.9GHz, which indicates the efficiency of the structure. The vertical notch of D_1 and D_2 is included at the surface plane. As shown in Fig. 2 (a), this structure modification from a single element to an array configuration offers an increase in bandwidth, thereby covering the frequency from the Ka-band. Fig. 2 (a) and Fig. 2 (b) gives the Return loss and Isolation of the MIMO antenna without meta surface.

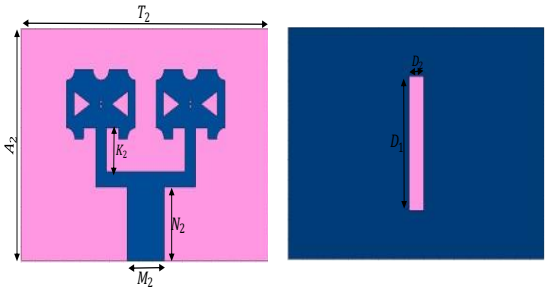

(b)

Figure 1. (B) Top And Bottom View Of 1x2 Element Antenna

The procedure is being developed to achieve MIMO performance. Fig. 1 (c) displays the four components are positioned at the opposite sides of a dielectric substrate with 30 mm x 43 mm x 0.787 mm size. Additionally, the rear surface includes uniform slots barely underneath MIMO configuration. The simulated return loss values for the MIMO antenna displayed in Fig. 3 (a) presents similar nature, at Ka-band resonant frequency. This shows that the MIMO antenna bandwidth is narrower than the two-element array. The near-field coupling effects are often responsible for this little bandwidth loss. Fig. 3(b) illustrates the isolation between elements 1 & 2 and also between elements 3 & 4.

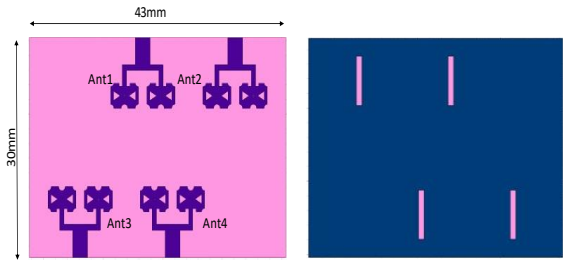

(c)

Figure 1. (C) Top And Bottom View Of 4- Port MIMO Antenna

Table 1. Optimal Design Specifications (In Mm).

Parameter	Value	Parameter	Value
Single element parameter			
A_1	9.5	K_1	2.2
T_1	7.7	M_1	1.7
R_1	4.7	S_1	0.2
U_1	2.4	I_1	0.2
N_1	1.2	H_1	0.2
I_2	1.3	H_2	1.3
S_2	1.3		
Two element array parameters			
K_2	2.2	N_2	3.7
A_2	11.7	M_2	2.5
T_1	17	D_1	6.8
D_2	1		
Unit cell of metamaterial			
E_1	0.7	E_2	0.7
Meta surface parameter			
C_1	1	C_2	1

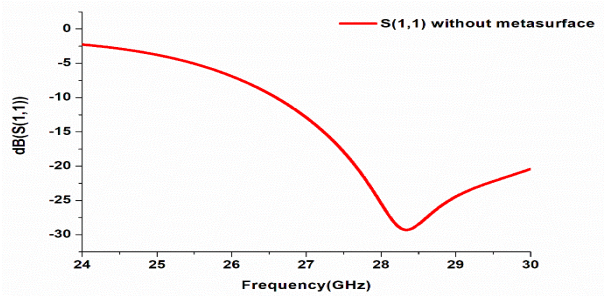

(a)

Figure 2. (a) Return Loss

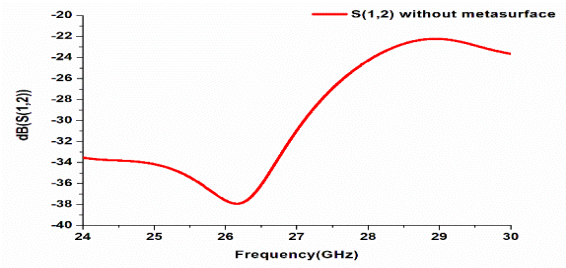

(b)

Figure 2. (B) Transmission Coefficient

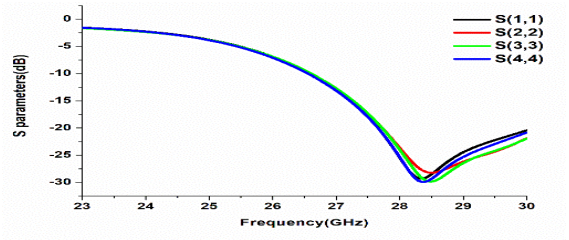

(a)

Figure 3. (A)Return Loss ($S_{11}, S_{22}, S_{33}, S_{44}$)

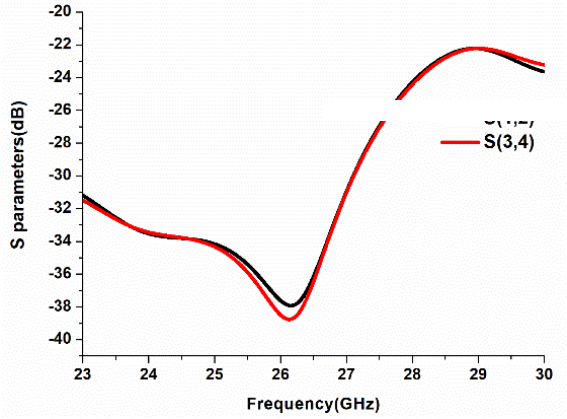

(b)

Figure 3. (B) Transmission Coefficient

The performance of the MIMO antenna in terms of reflected characteristics indicates the decayed behaviour mainly because of coupling problems. A meta surface is a useful process for enhancing the radiation efficacy in terms of operational bandwidth, isolation between MIMO parts and antenna gain.

A meta surface is just the periodic positioning of basic elements at a predetermined gap from one another. The primary element in this implementation is designed at 28.9 GHz. The dielectric substrate is Rogers Trademark 5880 with 2.2 as relative permittivity and height of 1.6 mm. The simulations of a unit cell are performed using HFSS in the time domain. The final optimized unit cell comprises two SSR with a rectangular geometrical design in the middle. Fig. 4(a)illustrates the unit cell. The unit cell is resonating at 28.9 GHz. Fig. 4(b) shows the arrangement of 9x6 SRR The transmission coefficient plot illustrates that at the resonant frequency, the basic element loss is virtual notifying that the entire transmission at the required band is guaranteed.

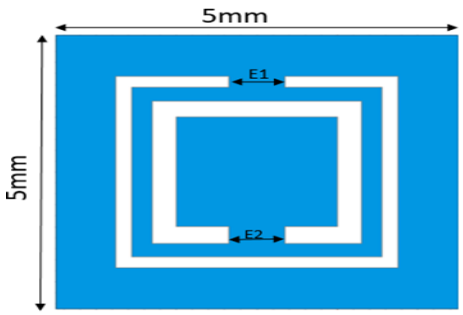

Figure 4. (a) Unit cell SRR

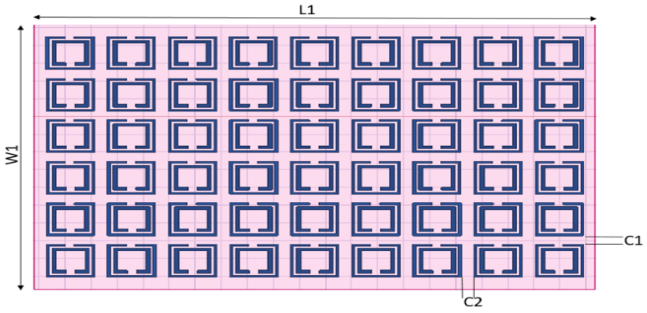

(b)

Figure 4. (B) Arrangement Of 9x6 Srr

At 28.9 GHz, both permeability and permittivity tend to be null value, suggesting that the refractive indexes are zero. After that, a Meta surface array is created by Stacking 9x6 primary elements with a gap of c1,c2, as shown in Fig. 4 (b) 30x43mm are the dimensions of the meta surface. To upgrade the efficacy of the antenna, the meta surface is stacked above the MIMO antenna at a distance of 5.75, as presented in Fig. 4(c). The MIMO antenna exhibit a considerable boost in performance after including meta surface.

(c)

Figure 4. (C)Side View of Antenna with Meta surface

Fig. 5(a) illustrates the improvement in impedance transmission capacity(bandwidth), spanning the frequency band in the Ka-band. Because of additional antenna have almost identical behaviour only Antenna1curve is displayed here. Fig. 5(b) illustrates the minimal isolation between Antenna1 and Antenna2 with meta surface, which is about -53.88dB. The Antenna1 and Antenna3 both have a minimal separation of -40 dB throughout the full working frequency spectrum. Antenna2 and Antenna4 exhibit the same behaviour. The coupling between the radiating components is decreased, while the isolation is greatly raised. Fig. 5(c)compares the simulated broadside gain of antenna at various frequencies in the working band at different stages of design advancement. The antenna gain is found to be higher.

In the first stage single element antenna converted into a 1x2 element array and later modified into a 4 element MIMO antenna, which improved the gain from 10.5 dB to 12.9 dB at 28.9 GHz. however, using a meta surface increases the gain by about 2.6dB. In this case, the meta surface functions as a superstrate layer, providing a resonant cavity action that increases the gain of the radiator. The isolation is also improved by stacking meta surface above the MIMO Antenna.

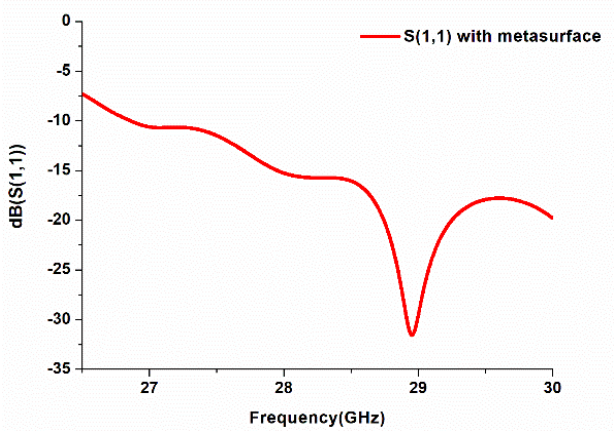

(a)

Figure 5. (A) Return Loss with Meta surface

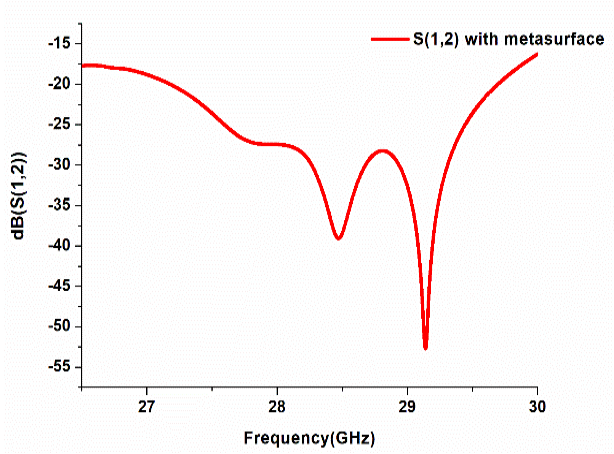

(b)

Figure 5. (B) Transmission Coefficient with Meta surface

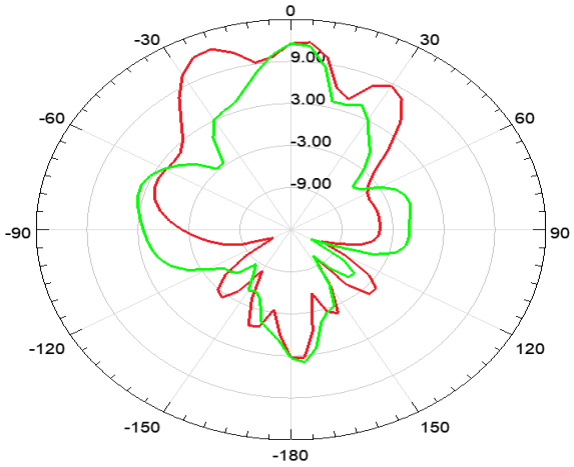

(c)

Figure 5. (C) Radiation Pattern

3. Memo Performance

Different characteristics, such as DG, CCL, ECC, MEG are extremely important for assessing a MIMO efficiency. These factors are explained further.

3.1 ECC [Envelope correlation Coefficient]

The ECC measures the degree of separation between the two antenna emission patterns. The ECC is reported to be lower than the accepted value of 0.5. The formula to compute ECC is as follows given in[1]. Fig. 6(a) illustrates the plots of ECC between the antennas. The ECC obtained is below 0.5.

$$\rho_{ec,ij} = \frac{\left|S_{ii} * S_{ij} + S_{ji} * S_{jj}\right|^2}{\left(1 - |S_{ii}|^2 - S_{ij}{}^2\right)\left(1 - \left|S_{ji}\right|^2 - S_{jj}{}^2\right)}$$

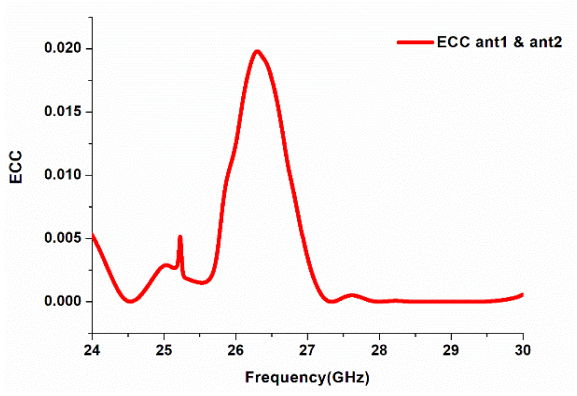

(a)

Figure 6. (A)ECC Plot Between Antenna 1 And Antenna 2.

3.2 Dg [Diversity Gain]

Another important MIMO system performance is diversity gain. It shows how much transmit power is reduced after utilising a diversity strategy. The DG accepted value is 10dB. The relationship is used to calculate diversity gain [1].Fig. 6(b) illustrates the diversity gain between antennas which is nearly 9.98dB.

$$D_{iG} = 10\sqrt{1 - \left|\rho_{ec,ij}\right|^2}$$

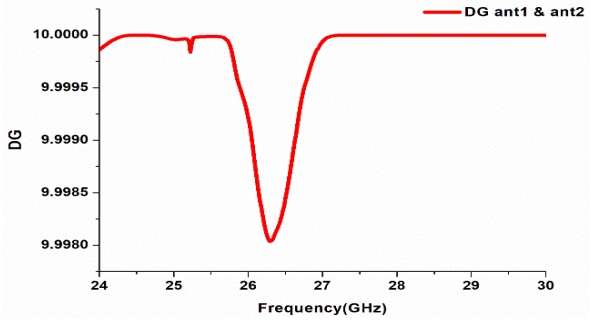

(b)

Figure 6. (B)DG Plot Between Antenna 1 And Antenna 2.

3.3 Meg [Mean Effective Gain]

Mean Effective Gain, which seems to be the mean acquired power to mean input power.

$$ME_f G=0.5\left(1-\sum_j^k S_{ij}\right)$$

For optimal diversity performance, the standard value of the Mean effective gain $\boldsymbol{ME_f G}$ should be[1].

$$-3 \text{ dB} \leq ME_f G \leq -12 \text{ dB}.$$

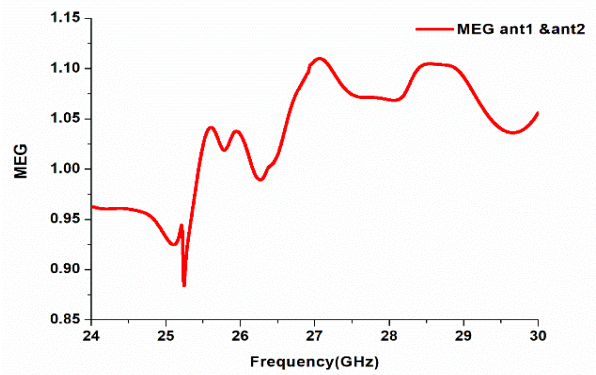

(c)

Figure 6. (C)MEG Plot Between Antenna 1 and Antenna 2.

3.4 CCL [Channel Capacity Loss]

In theory, the channel capacity of a MIMO system rises as the count of antenna components increases. Due to the correlation seen between MIMO connections [1]. The accepted value is 0.4 bit/s/Hz. Fig. 6. (d) illustrates the CCL between the antennas, it is shown clearly which is below the acceptance value.

$$\text{C(loss)} = -log_{10}\det(a_k)$$

Where a_k is correlation Matrix

$$a_k = \begin{bmatrix}\sigma_{11}\sigma_{11}\\ \sigma_{21}\sigma_{22}\end{bmatrix}$$

where,

$$\sigma_{ii} = 1-\left(|S_{ii}|^2-|S_{jj}|^2\right)$$

$$\sigma_{jj} = 1-\left(S_{ii}*S_{ij}+S_{ji}S_{jj}{}^*\right)$$

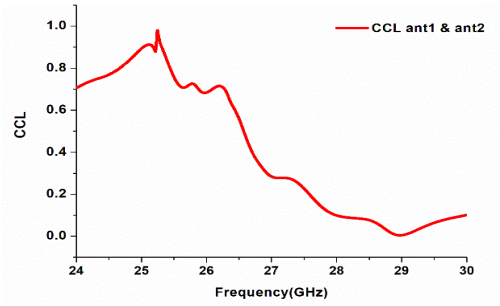

(d)

Figure 6. (D)CCL Plot Between Antenna 1 And Antenna 2

4. Comparing Results with Related Work

Table 2 displays the comparison of the proposed antenna and other published works in the recent past. The suggested MIMO antenna with a metasurface array with respect to the amount of isolation exceeds the previously published research. Furthermore, the presented MIMO antenna has a much larger gain than [20], [21], [22], [24],[26]. In comparison to the previous antennas covered here, the given antenna design exhibits superior MIMO efficiency. Hence the suggested MIMO antenna is the most appropriate choice for present and future wireless technologies.

Table 2. Comparing Results with Related Work

Ref	No. of ports	Optimization techniques	f_c(GHz)	Gain (dB)	Isolation (dB)	ECC (dB)	CCL (Bits/Sec/Hz)
[11]	2	MIMO+ Meta surface	28	16-17	-37	Not Calculated	Not Calculated
[13]	2	MIMO+EBG	28,38	11.5, 10.9	-20	<0.12	Not Calculated
[20]	4	MIMO+FSS	30	Not Provided	-25	Not Calculated	Not Calculated
[21]	4	MIMO+DGS	28	8.3	-17	<0.5	<0.4
[22]	1	Metamaterial	26	7.4	N/A	N/A	N/A
[23]	2	array MIMI+EBG	24	6	-37	0.24	Not Calculated
[24]	4	DRA-BASED MIMO+ Metamaterial	28	7	-29.34	0.02	Not Calculated
[25]	2	MIMO+ Metamaterial based PR wall	60	Not Provided	-22	$<0.1e^{-6}$	Not Calculated
[26]	4	MIMO+ Metamaterial	26	10.27	-45	$<0.1e^{-6}$	<0.4
This work	4	MIMO+ Metamaterial	28.9	12.9	-53.88	$<0.1e^{-6}$	<0.4

5. Conclusion

A Broadband Meta surface based MIMO antenna with better gain and isolation characteristics for 5G Millimetre wave system is presented. A single antenna is transformed into an array configuration to improve gain. As a result, each MIMO antenna is made up of a 1x2 element array supplied by a concurrent feedline. A 9x6 Split Ring Resonator (SRR) elongated cell is stacked above the antenna to improve gain and eliminate the coupling effects between the MIMO components. This developed antenna is designed to operate at Ka-band. Furthermore, placing the meta surface above the MIMO antenna at a height of about 5.75 optimizes the gain by 2.6 dBi and isolation between the elements. with a highest recorded gain of 12.9 dBi. Therefore, the investigation of MIMO with low ECC and CCL displayed high diversity performance. This proves that the suggested MIMO is suitable for the execution of 5G mm-wave system.

References

[1] S. Tariq, S. I. Naqvi, N. Hussain and Y. Amin, "A Metasurface-Based MIMO Antenna for 5G Millimetre-Wave Applications," in IEEE Access, vol. 9, pp. 51805-51817, 2021, doi: 10.1109/ACCESS.2021.3069185.

[2] N. O. Parchin et al., "Eight-Element Dual-Polarized MIMO Slot Antenna System for 5G Smartphone Applications," in IEEE Access, vol. 7, pp. 15612-15622, 2019, doi: 10.1109/ACCESS.2019.2893112.

[3] B. Yu, K. Yang, C. Sim and G. Yang, "A Novel 28 GHz Beam Steering Array for 5G Mobile Device With Metallic Casing Application," in IEEE Transactions on Antennas and Propagation, vol. 66, no. 1, pp. 462-466, Jan. 2018, doi: 10.1109/TAP.2017.2772084.

[4] K. S. Sultan, H. H. Abdullah, E. A. Abdallah and H. S. El-Hennawy, "Metasurface-Based Dual Polarized MIMO Antenna for 5G Smartphones Using CMA," in IEEE Access, vol. 8, pp. 37250-37264, 2020, doi: 10.1109/ACCESS.2020.2975271.

[5] T. S. Rappaport et al., "Millimetre Wave Mobile Communications for 5G Cellular: It Will Work!," in IEEE Access, vol. 1, pp. 335-349, 2013, doi: 10.1109/ACCESS.2013.2260813.

[6] Wei, R. Q. Hu, Y. Qian, and G. Wu, ‘‘Key elements to enable millimetre wave communications for 5G wireless systems,’’ IEEE Wireless Commun., vol. 21, no. 6, pp. 136–143, Dec. 2014.

[7] P. Gao, S. He, X. Wei, Z. Xu, N. Wang and Y. Zheng, "Compact Printed UWB Diversity Slot Antenna With 5.5-GHz Band-Notched Characteristics," in IEEE Antennas and Wireless Propagation Letters, vol. 13, pp. 376-379, 2014, doi: 10.1109/LAWP.2014.2305772.

[8] S. Tripathi, A. Mohan, and S. Yadav, "A compact koch fractal UWB MIMO antenna with WLAN band-rejection," IEEE Antennas and Wireless Propagation Letters, vol. 14, pp. 1565-1568, 2015.

[9] Y. Li, C.-Y.-D. Sim, Y. Luo, and G. Yang, "12-Port 5G massive MIMO antenna array in sub-6GHz mobile handset for LTE bands 42/43/46 applications," IEEE Access, vol. 6, pp. 344-354, 2018.

[10] A. Li, S. Singh, and D. Sievenpiper, ‘‘Metasurfaces and their applications,’’ Nanophotonics, vol. 7, no. 6, pp. 989–1011, 2018.

[11] M. Akbari, H. Abo Ghalyon, M. Farahani, A. Sebak and T. A. Denidni, "Spatially Decoupling of CP Antennas Based on FSS for 30-GHz MIMO Systems," in IEEE Access, vol. 5, pp. 6527-6537, 2017, doi: 10.1109/ACCESS.2017.2693342.

[12] S. Gupta, Z. Briqech, A. R. Sebak, and T. A. Denidni, ‘‘Mutual-coupling reduction using metasurface corrugations for 28 GHz MIMO applications,’’ IEEE Antennas Wireless Propag. Lett., vol. 16, pp. 2763–2766, 2017.

[13] M. Farahani, J. Pourahmadazar, M. Akbari, M. Nedil, A. R. Sebak, and T. A. Denidni, ‘‘Mutual coupling reduction in millimetre MIMO antenna array using a metamaterial polarization-rotator wall,’’ IEEE Antennas Wireless Propag. Lett., vol. 16, pp. 2324–2327, 2017.

[14] C. A. Balanis, *Antenna Theory: Analysis and Design*, 3rd ed. Hoboken, NJ, USA: Wiley, 2005.

[15] O. Yurduseven, D. Smith, and M. Elsdon, ‘‘Printed slot loaded bow-tie antenna with super wideband radiation characteristics for imaging applications,’’ *IEEE Trans. Antennas Propag.*, vol. 61, no. 12, pp. 6206–6210, Dec. 2013.

[16] M. R. Islam, ‘‘Study and implementation of wideband bow-tie antennas,’’ M.S. thesis, Georgia Southern Univ., Statesboro, GA, USA, 2017.

[17] S. Rangan, T. S. Rappaport, and E. Erkip, ‘‘Millimetre-wave cellular wireless networks: Potentials and challenges,’’ *Proc. IEEE*, vol. 102, no. 3, pp. 366–385, Mar. 2014.

[18] T. J. Cui, D. Smith, and R. Liu, *Metamaterials: Theory, Design, and Applications*. New York, NY, USA: Springer, 2009.

[19] N. Hussain, M.-J. Jeong, J. Park, and N. Kim, ‘‘A broadband circularly polarized Fabry–Perot resonant antenna using a single-layered PRS for 5G MIMO applications,’’ *IEEE Access*, vol. 7, pp. 42897–42907, 2019.

[20] D. Sievenpiper, ‘‘Metasurfaces and their applications,’’ *Nanophotonic*, vol. 7, no. 6, pp. 989–1011, 2018. A. Li, S. Singh,

[21] M. Khalid, S. I. Naqvi, N. Hussain, M. Rahman, Fawad, S. S. Mirjavadi, M. J. Khan, and Y. Amin, ‘‘4-port MIMO antenna with defected ground structure for 5G millimetre wave applications,’’ *Electronics*, vol. 9, no. 1, p. 71, Jan. 2020.

[22] A. A. R. Saad and H. A. Mohamed, ‘‘Printed millimetre-wave MIMObased slot antenna arrays for 5G networks,’’ *AEU Int. J. Electron. Commun.*, vol. 99, pp. 59–69, Feb. 2019.

[23] H. Jiang, L.-M. Si, W. Hu, and X. Lv, ‘‘A symmetrical dualbeam bowtie antenna with gain enhancement using metamaterial for 5G MIMO applications,’’ *IEEE Photon. J.*, vol. 11, no. 1, pp. 1–9, Feb. 2019.

[24] A. Iqbal, A. Basir, A. Smida, N. K. Mallat, I. Elfergani, J. Rodriguez, and S. Kim, ‘‘Electromagnetic bandgap backed millimetre-wave MIMO antenna for wearable applications,’’ *IEEE Access*, vol. 7, pp. 111135–111144, 2019.

[25] S. Gupta, Z. Briqech, A. R. Sebak, and T. A. Denidni, ‘‘Mutual-coupling reduction using metasurface corrugations for 28 GHz MIMO applications,’’ *IEEE Antennas Wireless Propag. Lett.*, vol. 16, pp. 2763–2766, 2017

[26] S. Tariq, S. I. Naqvi, N. Hussain and Y. Amin, "A Metasurface-Based MIMO Antenna for 5G Millimetre-Wave Applications," in IEEE Access, vol. 9, pp. 51805-51817, 2021, doi: 10.1109/ACCESS.2021.3069185.

[27] N. S. Murthy, ‘‘Improved isolation metamaterial inspired mm-Wave MIMO dielectric resonator antenna for 5G application,’’ Prog. Electromagn. Res. C, vol. 100, pp. 247–261, Mar. 2020.

[28] A. Iqbal, A. Basir, A. Smida, N. K. Mallat, I. Elfergani, J. Rodriguez, and S. Kim, ‘‘Electromagnetic bandgap backed millimetre-wave MIMO antenna for wearable applications,’’ IEEE Access, vol. 7, pp. 111135–111144, 2019.

[29] A. A. R. Saad and H. A. Mohamed, ‘‘Printed millimetre-wave MIMObased slot antenna arrays for 5G networks,’’ AEU Int. J. Electron. Commun., vol. 99, pp. 59–69, Fe

[30] M. Akbari, H. A. Ghalyon, M. Farahani, A.-R. Sebak, and T. A. Denidni, ‘‘Spatially decoupling of CP antennas based on FSS for 30-GHz MIMO systems,’’ IEEE Access, vol. 5, pp. 6527–6537, 2017.

[31] M. Farahani, J. Pourahmadazar, M. Akbari, M. Nedil, A. R. Sebak, and T. A. Denidni, ‘‘Mutual coupling reduction millimetre-water wave MIMO antenna array using a metamaterial polarization-rotator wall,’’ IEEE Antennas Wireless Propag. Lett., vol. 16, pp. 2324–2327, 2017.

[32] M. Khalid, S. I. Naqvi, N. Hussain, M. Rahman, Fawad, S. S. Mirjavadi, M. J. Khan, and Y. Amin, ‘‘4-port MIMO antenna with defected ground structure millimetre- water wave applications,’’ Electronics, vol. 9, no. 1, p. 71, Jan. 2020.

[33] ‘‘MIMO antennas for smart 5G applications,’’ IEEE Access, vol. 6, pp. 77014–77021, 2018.

[34] H. Jiang, L.-M. Si, W. Hu, and X. Lv, ‘‘A symmdual-beam dual beam bowtie antenna with gain enhancement using metamaterial for 5G MIMO applications,’’ IEEE Photon. J., vol. 11, no. 1, pp. 1–9, Feb. 2019.

[35] A novel architecture for the realization of IoT-enabled ecg signal quality assessment using wavelet decomposition for baseline wander removal, Defense S and T Technical Bulletin, 2018, 11(2), pp. 192–201.